MULTIPHYSICS SIMULATION OF MICROFLUIDIC REACTOR FOR POLYMERASE CHAIN REACTION

Barbaros Cetin[*] and İlbey Karakurt
[1] İhsan Doğramacı Bilkent University, Mechanical Engineering Department
Microfluidics and Lab-on-a-chip Research Group 06800 Ankara, Turkey
([*] Corresponding author: barbaros.cetin@bilkent.edu.tr)

ABSTRACT. Polymerase-chain-reaction (PCR) is a thermal cycling process (repeated heating and cooling of PCR solution) for amplifying DNA. PCR devices have many biomedical applications. One of the most important aspects for the success of PCR is to control the temperature of the solution precisely at the desired temperature levels required for PCR in a cyclic manner. Microfluidics offers a great advantage over conventional techniques since very small amounts of PCR solution is needed for the process to occur at the desired temperature levels. In this study, a multiphysics-based computational model is developed to assess the thermal performance of a microfluidics platform for continuous-flow PCR. The microfluidic platform consists of a spiral channel on a glass wafer with integrated chromium microheaters. The computational model couples the convection heat transfer and fluid flow within the microchannles and the electric field generated at the microheaters using COMSOL® Multiphysics software. With the current computational model, the effects of design parameter on the performance of PCR cycle can be understood and utilized for the optimization of a microfluidic PCR device. Moreover, the computational model can also be implemented for a general design tool for the design of efficient microfluidics based thermal reactors which can extend the boundaries of microfluidics technologies in biomedical and bioengineering fields.

INTRODUCTION

Chemical and bio-reactors are used in various biological and chemical applications. The ability to increase the amount of DNA plays a vital role in many applications [Saiki et al. 1985]. One of the most widely used reactors for this purpose are Polymerase chain reaction (PCR) reactors [Zhang et al. 2006]. PCR is a thermal cycling process in which DNA is amplified to a desired level. A typical pre-defined thermal cycle can be summarized as follows:

(1) The first step is called denaturation and it enables the DNA structure to unfold and allows its strands to separate. The sample is heated to 90-96 °C for 20-30 seconds in this step.
(2) The second step is called the annealing and at this step the primers attach to their target strands on the DNA. The sample is cooled to 50-65 °C.
(3) The third step allows the replication of the double-strands and the elongation of the newly copied DNA. The sample is heated to around 72 °C for this step.

These steps are repeated 20-40 times to reach the required amplification level [Salemmilani and Cetin 2013, Hu et al 2006]. The reactors used for this reaction are generally used for clinical purposes of identifying organisms or infections that are currently being hosted by a human being. It should be noted that these are not the only fields of application the PCR

reactors can be used in, any application that requires a rapid increase in the amount of DNA/RNA are prospective applications where these devices can be used [Zhang et al. 2006]. The first silicon based PCR chip was introduced by Northrup et al [1993], and many research groups since that day have been working on this topic. The PCR-CE (CE: capillary electrophoresis) microfluidic chip was introduced in 1996, and research efforts still continue on in this area [Zhang and Xing 2007]. For the PCR to be performed effectively the sample has to go through a pre-defined heat cycle. At this point microfluidic PCR devices is a good option since minute amount of sample can be heated and cooled very fast enabling low consumption of sample material. Different PCR devices can be found in the literature such as chamber-based microfluidics PCR reactors and continuous-flow microfluidics PCR reactors [Zhang et al. 2006]. In the first type, the sample that will be amplified is kept inside a chamber where it is heated and/or cooled. In the second type, the sample flows through a microchannel network in which it experience different temperature zones. Typically these temperature zones are generated via heaters placed strategically at various locations on the microfluidics device. It should be noted that the stationary chamber reactors are not as effective as the continuous-flow reactors since the thermal mass in the first type is higher, and heating/cooling rates are slower which may lead to decreased amplification performance. There are different geometries and designs for the channels and the heaters that have been studied by research groups till now [Zhang and Xing 2007]. The first PCR reactor had a serpentine channel geometry which was not sufficient in allowing the sample to go through the pre-defined thermal cycle [Kopp 2005]. Research showed that PCR reactors with spiral channel geometry would be more effective in satisfying the thermal cycle [Zhang et al. 2006, Zhang and Xing 2007, Salemmilani and Cetin 2013, Xiaoyu et al 2007]. Another important parameter in designing a PCR reactor is the heating method. The heating methods employed in the design of PCR reactors are generally investigated under two categories: contact heating, and non-contact heating. Thin film heaters are processed onto the PCR reactor either with micro machining or thin film deposition techniques. These types of contact heaters have small thermal masses and can heat up or cool down in very small time intervals [Zhang and Xing 2007]. Apart from thin film heaters metal blocks or thermoelectric devices can be used in PCR reactors. In these types of PCR reactors, the thermal mass is higher when compared to thin film heated PCR reactors. Thus, they are not as effective as the thin film heater, and consume more energy compared to this. [Zhang and Xing 2007]. The PCR device modelled and analyzed in this study utilizes spiral channel geometry. In this design approach, the three pre-defined temperature zones is created by three thin film heaters which are deposited to a glass surface. Previously, it has shown that spiral geometry is successful to generated required thermal cycling. In this study, a multi-physic based numerical model which predicts temperature cycling of a buffer solution within a continuous-flow microfluidic PCR reactor. Actually, numerical modeling is not a common tool for the design of microfluidic PCR reactors. In a previous study, same group developed a numerical model to predict the performance of a microfluidic PCR reactor [Salemmilani and Cetin 2013]. In this aforementioned study, the temperature and the flow field was coupled the thermal energy generated in the heaters was modeled as an isoflux thermal boundary condition. In this study, the model is extended to model the heating at the heater electrodes by modeling the electric field and the Joule heating within the electrodes. Moreover, the fluid flow and the temperature field within the microfluidic channel is modeled by using the pipe flow module of the COMSOL® Multiphysics which leads to an efficient computational model in terms of computational time and memory requirement. Utilizing the proposed computational model, performance of a new serpentine heater design is also discussed.

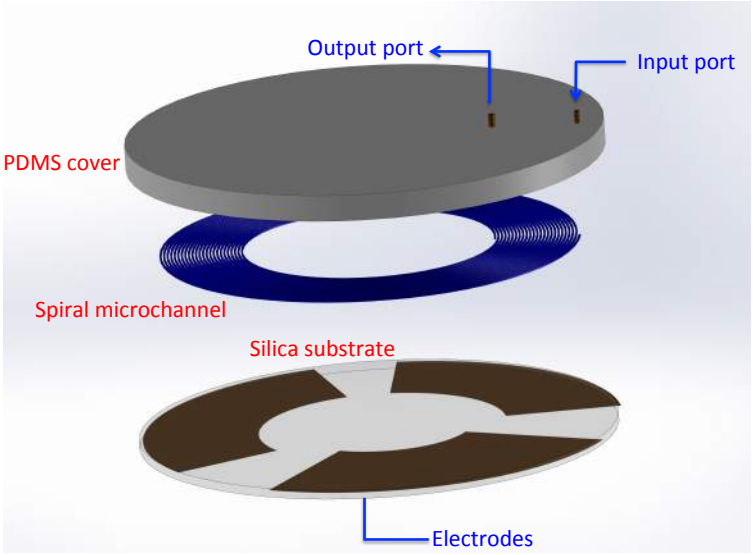

Figure 1. Schematic drawing of the microfluidic PCR reactor

ANALYSIS

For the purposes of this study, a spiral channeled PCR reactor is modelled to observe the effects of an applied electric field to the heaters on the performance of the thermal cycle. A schematic drawing of the system can be seen in Fig 1. The system composed of a silica substrate and a PDMS cover. The spiral network is embedded in the PDMS. The heaters are deposited on the bottom side of the silica substrate. There are three different electrode regions to create the three different temperature zones required for the PCR. A schematic drawing of the configuration of the three heaters together with some design parameter can be seen in Fig. 2. The flow of the buffer solution starts from the input port, and follows the spiral channel towards the outer port. Typically 20-40 cycles are required for the PCR. In this study, 24 cycles are used. Two different cases are simulated using the electrode configuration in Fig. 1. As a third case, the heating performance of a serpentine heater is assessed. The geometric parameters that are considered in the first two cases, namely **Case-1** and **Case-2** can be found in Table 1.

Table 1
Geometric Parameters for the first two cases

Design Par.	Case 1	Case 2
θ_1	15°	30°
θ_2	105°	95°
θ_3	20°	30°
θ_4	105°	80°
θ_5	10°	20°
r_1	8.8 mm	7.0 mm
r_2	8.8 mm	5.1 mm

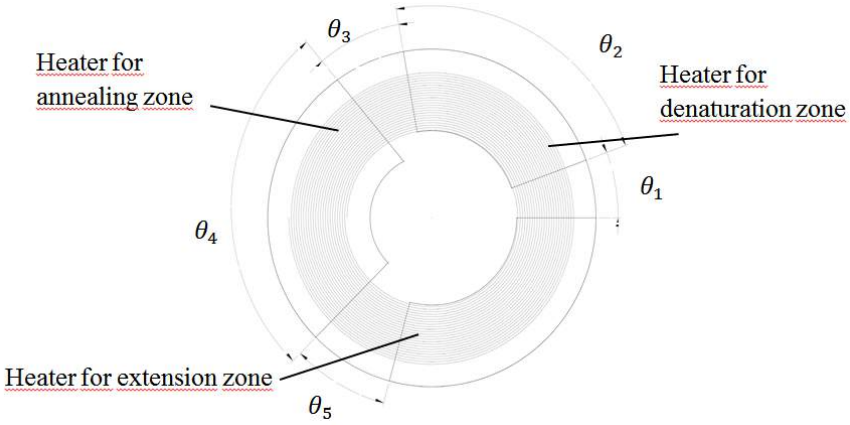

Figure 2. Schematic drawing of heaters

To obtain the fluid and temperature field within the microchannel network, Navier-Stokes equation together with the energy equation need to be solved. However, due to the different length scales of the problem, to resolve the flow and temperature field with a reasonable accuracy, large number of mesh is needed (the width of the microchannel is 100 μm with a length of approximately 2m). One alternative to get the flow and the temperature field with a reasonable accuracy is to utilize Pipe-flow Module of COMSOL® Multiphysics software. In this module, average velocity and average temperature within the microchannel network is obtained by using 1D momentum and energy balance over the control volumes generated along the path of a pipe together with the correlations for the friction factor and the heat transfer coefficient. The governing equations for the 1D continuity, momentum and energy equation can be written as:

$$\nabla_t \, AC_p u\mathbf{e}_t = 0 \tag{1}$$

$$0 = -\nabla_t p \cdot \mathbf{e}_t - \frac{1}{2} f_D \frac{\rho}{d_h} |u| u + F \cdot \mathbf{e}_t \tag{2}$$

$$\rho AC_p u\mathbf{e}_t \cdot \nabla_t T = \nabla_t \cdot (Ak\nabla_t T) + \frac{1}{2} f_D \frac{\rho A}{d_h} |u| u^2 + Q_{wall} \tag{3}$$

where t represents the tangential direction, $\boldsymbol{e_t}$ is the unit normal vector in the tangential direction, f_D is the friction factor, u is the average velocity in the tangential direction, and T is the average temperature in the tangential direction. Q_{wall} (W/m) represents the external heat exchange through the pipe wall and is seen as a source term in the energy equation. Q_{wall} can be defined as:

$$Q_{wall} = (hZ)_{eff}(T_{ext} - T) \tag{4}$$

in which $(hZ)_{eff}$ is the effective heat transfer coefficient where Z(m) is the wall perimeter of the pipe, and T_{ext} is the external temperature obtained via the heat transfer equation. The boundary conditions for the solution of Eqns. (1)-(3) can be stated as: uniform volumetric flow rate and specified temperature at the inlet, heat outflow and zero pressure boundary

condition at the outlet. The volumetric flow rate at the inlet is assigned to ensure the buffer solution flows through the specified temperature zones at the specified intervals throughout the spiral microchannel network.

The temperature field within the silica substrate and the PDMS cover is governed by the conduction equation:

$$\rho C_p \mathbf{u} \cdot \nabla T = \nabla \cdot (k \nabla T) + Q \tag{5}$$

Heating is modelled by an applied electric field across each heater. The electrical field needs to be determined within the electrodes. These electrodes will be deposited onto the silica substrate during the fabrication of the device. Typical deposition thickness will be around 300nm. To model 3D geometry with a thickness of 300nm requires large amount of mesh. Therefore, the electric field and the resulting Joule heating are modeled by using an electrical shell model. In this model, the governing equation is the Laplacian equation as:

$$\nabla_t \cdot (-d\sigma \nabla_t V) = 0 \tag{6}$$

where d is the thin layer's thickness (m), σ is the electrical conductivity (S/m), V is the electric potential (V), and t denotes the tangential direction. To model the heat transfer in the thin conducting layer, highly conductive layer feature of the General Heat Transfer interface is used which does not require any separate interface introduction. The heat generated as a result of Joule heating (in W/m^2) within the thin layer can be obtained by:

$$q_{prod} = dQ_{DC} \tag{7}$$

$$Q_{DC} = J \cdot E = \sigma |\nabla_t V|^2 \left(\frac{W}{m^3}\right) \tag{8}$$

where Q_{DC} is the power density (which is the heat generated as a result of the Joule heating within the heater electrode). The generated heat appears as an inward heat flux boundary condition at the interface of the silica substrate and the heaters. Convective cooling with a heat transfer coefficient of $2\ W/m^2K$ is assigned as a thermal boundary condition for all other boundaries. Once the temperature and the flow field within the microchannel are obtained, the average temperature can be plotted as a function of time (by dividing the average temperature by the average velocity within the spiral microchannel) to check whether the thermal cycling satisfies the condition for a successful PCR.

NUMERICAL MODELING

COMSOL® Multiphysics, is a powerful, finite element method based multiphysics software with a Pipe-flow Module to model the flow in a long tubular structures, and electrical shell model to model electrical field within thin layer of structures. Therefore, COMSOL is used to model temperature, flow, and electric fields within the microfluidic reactor. Pipe-flow Module is utilized to obtain the average velocity and the average temperature inside the spiral microfluidic network. Heat Transfer in Solids Module is utilized to obtain the temperature

field within the silica substrate and the PDMS cover. AC/DC Module is used to model the electrical heat generation within the thin-film electrodes. Water is used as the material for the buffer solution, and chromium is used for the material of the electrodes. Material thermo-physical properties are temperature dependent. Therefore, all three modules are coupled. However to relax the solutions, first the coupled solution of the electric and temperature fields are obtained by assuming no flow condition within the microchannel. After this step, the flow field and temperature field inside the microchannels are obtained together with the pre-obtained temperature field. An iterative procedure is then used to obtain the converged solutions. The simulations were realized on a SuperServer Workstation (Intel Xeon X5687, Quad core, 3.60GHz, 96GB RAM). Pipe-flow Module allows the microchannels to be represented as 2D drawings inside the 3D geometry by assigning the geometry details (channel width, height, and shape) internally while solving the governing equations. This procedure reduces computation time since it does not require any 3D mesh to resolve the velocity and the temperature field within the microchannel. In the current model approximately 154000 elements are used. The approximate run time of this model is found to be around 5 minutes (including all the iterations, typically three iterations is found to be enough). Both the computational time and the degrees of freedom for the coupled reduced dramatically. In our previous study [Salemmilani and Cetin 2013], where we solved the full Navier-Stokes equation together with the energy equation (i.e. convection equation) within the microchannel, the degree of freedom was approximately 1 million, and the typical computational time was around 20 minutes which did not include modeling of the electrical field within the electrodes.

RESULTS AND DISCUSSION

A multiphysics computational model is developed to predict the thermal cycle of microfluidic PCR reactor. As an extension to a study from our group, the generated heat as a result of the Joule heating is also included in the model. To determine the average temperature and the velocity of the buffer solution within the spiral microchannel network PFM is implemented. Implementation of the PPM reduced the computational time and the degree of freedom of the system significantly. In our previous study where we solved the full Navier-Stokes equation together with the energy equation (i.e. convection equation) within the microchannel, the degree of freedom was over 1 million (which did nit include the modeling of electrical field and Joule heating within the electrodes) and the computational time (excluding the modeling and meshing) was around 20 minutes. In this proposed model, it is found that number of degree of freedom is about 154000 and a typical computational time is around 5 minutes.

To recover the results form our previous study, **Case-1** and **Case-2** (which are the cases with the same geometric, fluidic and thermal input parameters with the previous study) are simulated. To obtain the desired temperature zones, three different voltage values are found (in our previous studies iso-flux thermal boundary conditions were tuned to get the desired the temperature zones). The temperature distribution on the microfluidic device and the average temperature of the buffer solution within the spiral microchannel network can be seen in Figs. 3 and 4 for **Case-1** and **Case-2**, respectively. As seen from the figures, three temperature zones and the cyclic behavior for the buffer solution can be obtained successfully. However, when the average temperature is inspected, it is clear that not all the cycles are within the acceptable temperature levels. There is a significant temperature gradient as the buffer solution flow to the center (i.e. significant deviations occur between the inlet and the outlet of

the reactor). These gradients can be seen as red dashed lines in the figures. The gradient is reduced in **Case-2** with the decrease in the inner radius of the denaturation zone's heater, and with the change in the angles between the three heaters. The increase in the angles between the heaters enabled less interference between the three different temperature zones. This temperature gradient was also observed in our previous study. However, it was not severe like in this case. The major reason for this temperature gradient is the result of the non-uniform electrical field over the electrodes which creates non-uniform Joule heating. Therefore, the heat flux generated within the electrodes is not uniform the electrodes which creates non-isoflux thermal boundary condition. To illustrate this the electric field over the electrodes are shown in Fig. 5. However, since the voltage values are different at each electrode, the resulting electric field values are different. Therefore, the electric field is normalized with the maximum value for each zone to demonstrate the distribution of the electric field over the electrodes. As seen from the figures, electric field is not uniform which leads to a non-uniform heating of the electrode. Therefore, it can be concluded that modeling the heaters as a the isoflux thermal boundary condition is not realistic since the electric field is not uniform within the electrodes which makes the inclusion of the modeling of the electric field a necessary step for more realistic simulations.

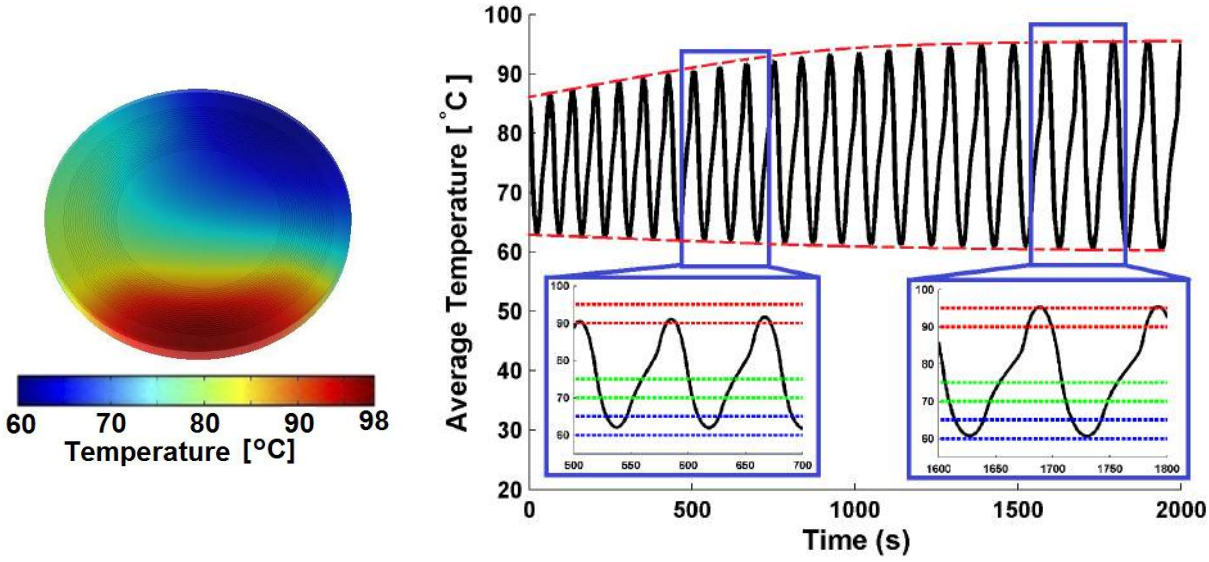

(a) **(b)**

Figure 3. **(a)** The temperature distribution on the microfluidic device, **(b)** the average temperature of the buffer solution within the spiral microchannel network (**Case-1**)

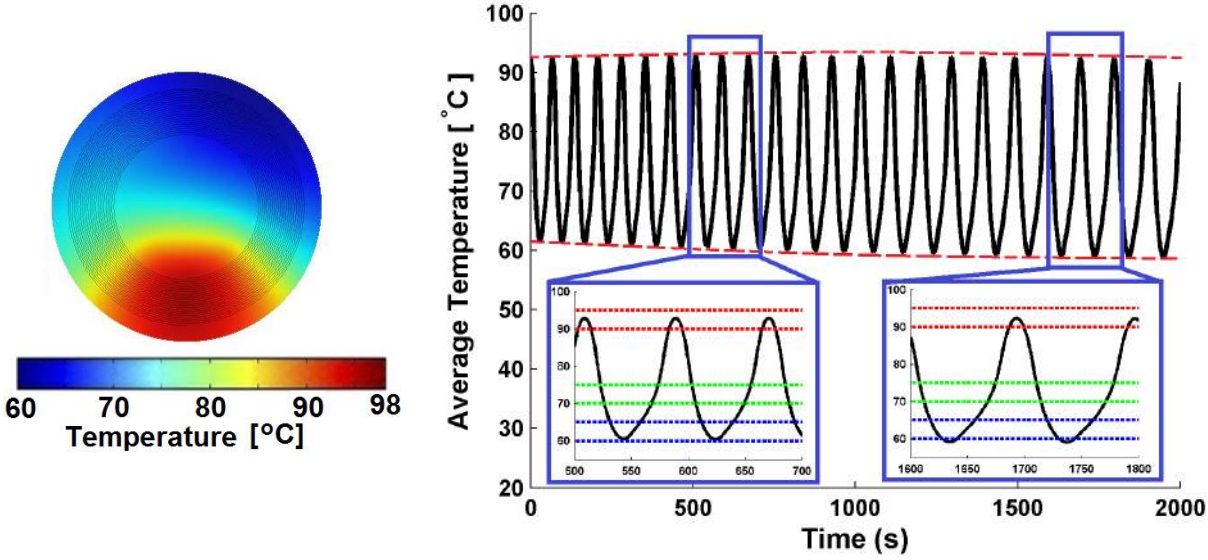

(b) **(b)**

Figure 4. **(a)** The temperature distribution on the microfluidic device, **(b)** the average temperature of the buffer solution within the spiral microchannel network (**Case-2**)

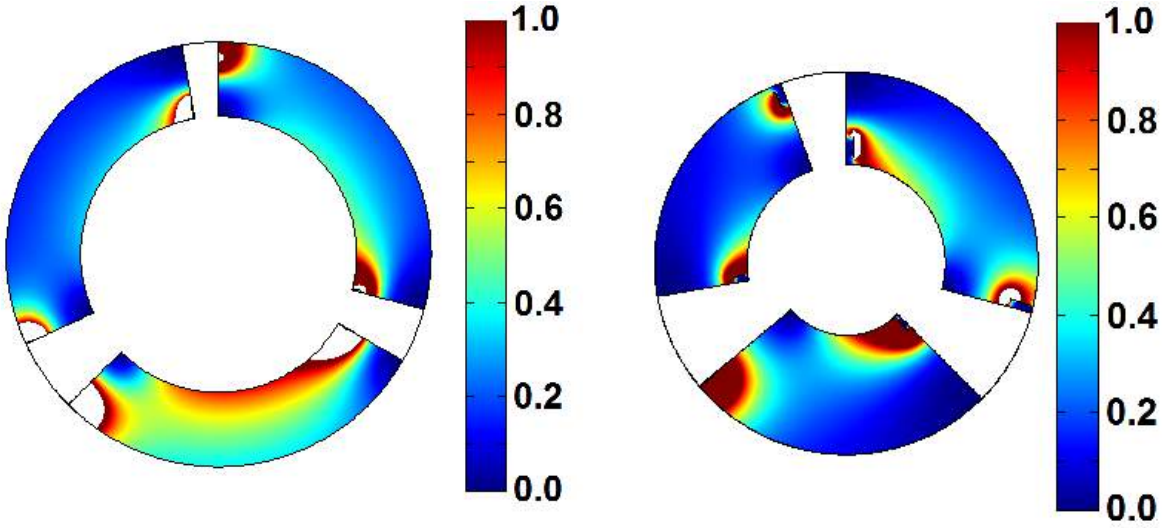

(a) Case-1 **(b)** Case-2

Figure 5. Electric field distribution over the electrodes

Another important issue with **Case-1** and **Case-2** is that, although the temperatures are within the desired temperature limits, the temperature is changing in each zone. A temperature plateau at each temperature zone is actually something that is desired for PCR. To achieve this, two and three piece electrodes were proposed previously [Salemmilani and Cetin 2013]. In this study, a serpentine heater is proposed (the drawing of the serpentine heaters can be seen in Fig. 6). In this configuration, electrical current follows the path of the electrodes,

which makes the electrical field more uniform than that of the previous electrode configuration. The electric field distribution on the serpentine electrodes can be seen in Figure 6, and the resulted temperature field can be seen in Fig. 7. As seen from Fig. 6 electric field becomes more uniform which leads to a more uniform heating. This uniform heating contributes to the plateau-like behavior at each zone as seen in Fig. 7. However, still, the temperature gradients exist from inlet to the exit. Although the average temperature as a function of time is not ideal, the serpentine electrode geometry is more promising than the first two cases in terms of the plateau-like behavior at each zone. Actually, by adjusting the geometric parameters of the spiral heaters, better thermal cycling behavior can be obtained. However, the optimization of the serpentine heater is not performed in this study.

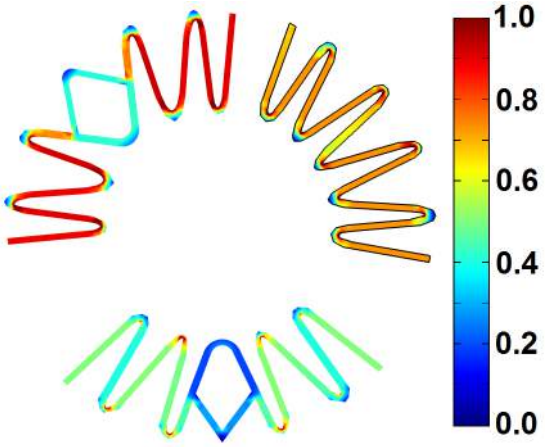

Figure 6. Electric field distribution over the serpentine electrodes

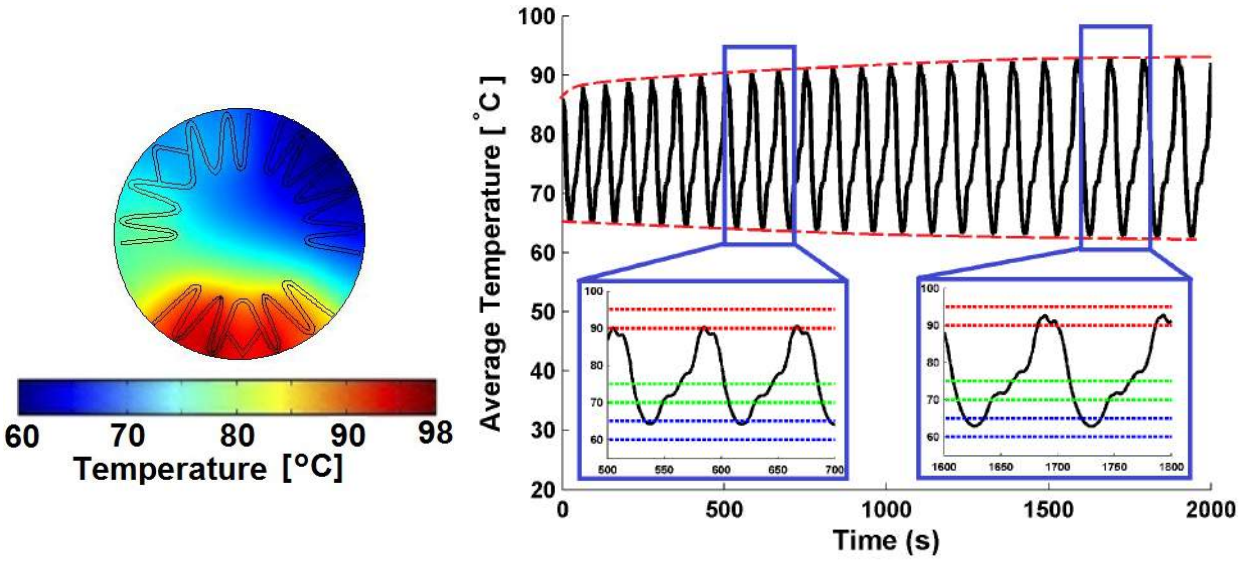

(a) **(b)**

Figure 7. **(a)** The temperature distribution on the microfluidic device, **(b)** the average temperature of the buffer solution within the spiral microchannel network

The proposed computational model has the ability to predict the thermal behavior of the microfluidic PCR reactor, and also gives an idea about the voltages values that need to be used during the practical implementation. Moreover, the computational model is computationally efficient which makes it a potential design tool for a microfluidic PCR reactor. Many different scenarios can be simulated, and the optimum design can be determined among these scenarios. The proposed computational methodology can also implemented for the modeling of any microfluidic thermal reactor.

SUMMARY AND FUTURE WORK

In this study, a multiphysics-based computational model is developed to predict the performance of a microfluidics thermal reactor with spiral microchannel network. The fluid flow, temperature, and electric field are simulated. By implementing the Pipe flow Module and the Electrical Shell Model, a computationally effective (both in terms of number of degree of freedom and computational time) model is developed. With this computational efficiency, the proposed model can be utilized a design tool for the design of a microfluidic PCR rector. Moreover, the proposed model can be implemented to any microfluidic system with the coupling of similar physics. The proposed computational model has also revealed that the replacement of the thin-film heaters with isoflux boundary condition does not give the whole physical picture.

At this point, the verification of the computational results is missing. The fabrication of the microfluidic PCR reactor and the experimental measurements of the temperature zones will be our future research direction. The fabrication of the electrodes will be performed by lithography-based deposition process, and the fabrication of the microfluidics channel will be performed by soft-lithography technique. The temperature measurements of the temperature zones will be either performed by infrared camera or by readings from the thermocouples located at some strategic locations. First phase of the study will be performed with the water-based buffer solution, and in the second phase of the experimentation, real PCR solution will be used.

ACKNOWLEDGMENT

Financial support from the Turkish Scientific and Technical Research Council, Grant No. 1919B011302937, is greatly appreciated.

REFERENCES

Hu, G., Xiang, Q., Fu, R., Xu, B., Venditti, R., and Li, D. [2006]. Electrokinetically controlled real-time polymerase chain reaction in microchannel using Joule heating effect, *Analytica Chimica Acta*, Vol. 557, No.1-2, pp. 146–151.

Kopp, M.U [2005], Chemical amplification: Continuous-Flow PCR on a Chip. *Science*, Vol.280, No.5366, pp.1046-1048.

Northrup, M. A., Ching, M.T., White, R.M. and Watson, R.T. [1993], Digest of Technical Papers: Transducers, *In Proc. the 1993 IEEE conference, New York*, pp. 924-926.

Saiki, R. K., Scharf, S., Faloona, F., Mullis, K. B., Horn, G. T., Erlich, H. A., and Arnheim, N., [1985]. Enzymatic amplification of beta globin genomic sequences and restriction site analysis for diagnosis of sickle cell anemia. *Science*, Vol. 230, No. 4732, pp. 1350–1354.

Salemmilani, R. and Cetin, B. [2013], Spiral microfluidics device for continuous flow PCR. In *Proc. ASME2013 Summer Heat Transfer Conf., Minneapolis, MN, USA, July 14-19.*

Xiaoyu, J., Zhiqiang, N., Wenyuan, C., and Weiping, Z. [2005]. Polydimethylsiloxane (PDMS)–based spiral channel PCR chip. *Electronics Letters*, No. 41, pp. 16.

Zhang, C., Xu J. , Ma, W., and Zheng, W., [2006], PCR microfluidic devices for DNA amplification, *Biotechnology Advances*, No. 24, pp.243-284.

Zhang, C., and Xing, D. [2007], Miniaturized PCR chips for nucleic acid amplification and analysis: latest advances and future trends, *Nucleic Acids Research*, Vol. 35, No.13, pp.4223-4237.